Journal of Thermal Analysis and Calorimetry (2018) 133:177–188
https://doi.org/10.1007/s10973-018-7398-1

Thermal analysis of ternary gypsum-based binders stored in different environments

Lenka Scheinherrová[1] · Magdaléna Doleželová[1] · Jakub Havlín[2] · Anton Trník[1,3]

Received: 2 November 2017 / Accepted: 21 May 2018 / Published online: 4 June 2018

Abstract
Although gypsum belongs to the low-energy environmentally friendly binders, its wider applications in building constructions are limited due to the negative effect of moisture on its mechanical properties. When calcined gypsum ($CaSO_4 \cdot 1/2H_2O$) transforms into its hydrated form ($CaSO_4 \cdot 2H_2O$), it is partially soluble in water and it has a relatively low strength. This problem can be resolved when gypsum is used as a part of binary or ternary binders. In this paper, a system consisting of calcined gypsum, lime, and silica fume is presented as a functional solution for a wider utilization of gypsum in wet environments. For this purpose, the newly designed materials were stored in different environments (laboratory conditions in air or water) up to 182 days. The effect of silica fume on the hydration process and the growth of the main products is evaluated by using differential scanning calorimetry and thermogravimetry in the temperature range from 25 to 1000 °C with a heating rate of 5 °C min^{-1} in an argon atmosphere. The carbonation level of studied materials is also evaluated. Besides this, the information about the thermal stability of studied materials is provided. These results are supported by evolved gas analysis, X-ray diffraction, and scanning electron microscopy. The basic physical and mechanical properties are determined to provide more detailed information about the behavior of the designed materials under various conditions at selected days of hydration. The addition of silica fume to the gypsum–lime system activates the pozzolanic reaction of the analyzed pastes, which is proved by the presence of the CSH phase and by the consumption of portlandite in the mixtures. Wet environment speeds up the hydration processes and prevents samples from carbonation.

Keywords Gypsum · Ternary binders · Silica fume · Thermal properties · Calorimetry

Introduction

Gypsum as a traditional building material has been used in building constructions since the days of the ancient Egypt, where it was used in pyramids. Actually, the oldest traces of gypsum applications are over 9000 years old. They were found in Syria and Anatolia [1]. Solid gypsum plaster and gypsum rock are calcium sulfate dihydrate with the chemical formula $CaSO_4 \cdot 2H_2O$. The manufacturing process, called calcination, involves driving the moisture out of the gypsum rock. The result of this process,

$$CaSO_4 \cdot 2H_2O \rightarrow CaSO_4 \cdot \frac{1}{2}H_2O + \frac{3}{2}H_2O, \quad (1)$$

is a white powder material, namely calcium sulfate hemihydrate ($CaSO_4 \cdot 1/2H_2O$) [2]. This reaction is reversible. Therefore, when calcium sulfate hemihydrate is mixed with water, the calcium sulfate dihydrate is formed again,

$$CaSO_4 \cdot \frac{1}{2}H_2O + \frac{3}{2}H_2O \rightarrow CaSO_4 \cdot 2H_2O. \quad (2)$$

Gypsum can be produced not only from natural gypsum mineral, but also from secondary raw materials, such as phosphogypsum [1, 3] or red gypsum. (The latter is a waste product from the titanium dioxide industry [4, 5].) The

✉ Lenka Scheinherrová
lenka.scheinherrova@fsv.cvut.cz

[1] Department of Materials Engineering and Chemistry, Faculty of Civil Engineering, Czech Technical University in Prague, Thákurova 7, 16629 Prague, Czech Republic

[2] Laboratory of Thermal Analysis, Central Laboratories, Institute of Chemical Technology, Technická 5, 16628 Prague 6, Czech Republic

[3] Department of Physics, Faculty of Natural Sciences, Constantine the Philosopher University in Nitra, A. Hlinku 1, 94974 Nitra, Slovakia

main difference between natural and chemically prepared gypsum is that the industrial gypsum has smaller crystals than the natural one, but both of them have the identical chemical composition [2]. The calcination of gypsum takes place at relatively low temperatures (100–120 °C), which is very beneficial for the environment. In addition, raw materials for the production of gypsum are cheap and relatively easily accessible. Gypsum also plays an important role in the cement production, although in small amounts (2.5–3.0 mass%). It is added into ground clinker to retard the rapid hydration of tricalcium aluminate (C_3A) to achieve better workability for longer duration. As a result of this reaction, ettringite is formed. Moreover, it was found out that gypsum accelerates the strength of blended cements in the early stages of hydration [6].

Despite these advantages, applications of gypsum in building construction are limited. The main disadvantage of gypsum application is in its low resistance against moisture. Gypsum is partially soluble in water and its strength decreases in wet environment. This problem can be eliminated if the calcined gypsum is a part of binary or ternary binders containing also a pozzolanic material and another element (e.g., lime), which can activate the pozzolanic reaction. One of the most frequently used pozzolanic material for this purpose is fly ash [7–9], which is probably given by the fact that it belongs to the most remarkable solid wastes in China, and therefore, its wider utilization is needed [9]. The properties of a mixture consisting of gypsum, lime, and fly ash can be improved with various types of pozzolan additions, such as expanded perlite or silica fume [10]. Silica fume is a pozzolan material with a very high surface area. The partial replacement of the fly ash by silica fume in the mixture gypsum–lime–fly ash (now, the system of four components) can improve the expansive phase formation of ettringite, which can cause cracking of the structure. So, mechanical properties decrease [10]. But this partial replacement helps to increase the bulk density which leads to a decrease in the open porosity. The formation of ettringite and the increase in bulk density are the main factors for an increase in thermal conductivity in the studied mixture. It was also found that silica fume can improve the pozzolanic reactions and the formation of cellular CSH structures [10]. The utilization of unconventional pozzolanic active materials, such as metakaolin, was also studied [11, 12]. The addition of metakaolin to gypsum–lime mixture improves the mechanical properties without a negative effect on thermal conductivity and water vapor diffusion properties [12]. Nevertheless, the above-mentioned research works are mainly focused only on the age of 7 and 28 days of hydration, and therefore, these results cannot provide the complex information about durability and structural changes of studied materials in a long-term horizon.

Gypsum itself is often used as a protection of various types of constructions against fire [13–16]. A high water content in the gypsum is the key to its high fire resistance because the calcination process starts when gypsum is exposed to the temperature above 80 °C, which leads to the release of water from gypsum. This water prevents the fire from penetrating the walls while it is evaporating [2]. This effect delays the development of the fire for a significant time. On the other hand, gypsum exposed to the high temperature exhibits significant shrinkage which can be eliminated by the addition of fillers [17]. While the behavior of gypsum at high temperature has been extensively studied, there is a lack of information about its performance in composed gypsum-based binders. Only a few research works were found up to date [17–22]. The mixture of gypsum–lime–silica fume shows better fire resistance than mixtures without silica fume. In addition, the samples without pozzolan are heavily damaged already at the temperature of 400 °C. The samples with silica fume exhibit cracking, but their integrity is still maintained [19]. In recent study [17], ternary gypsum-based pastes were enriched by fine fillers and then were exposed to high temperature of 1000 °C. It was found that samples made only from gypsum have better fire resistance properties then samples from gypsum–lime–silica fume. Nevertheless, obtained properties are still sufficient for normal usage, which is a promising result for the wider utilization of this environmentally friendly material. Therefore, a systematic research should be done in order to provide lacking information about the behavior of gypsum-based composites at high temperatures.

In this paper, the influence of high temperatures on the ternary gypsum-based system consisting of gypsum, lime, and silica fume is studied. Samples were stored for 35, 91, and 182 days in two different environments (laboratory conditions in air or water). After the chosen curing time, the thermal decomposition of the studied samples was investigated by a simultaneous thermal analysis in the temperature interval from 25 to 1000 °C with a heating rate of 5 °C min^{-1} in an argon atmosphere. The main products of hydration processes are identified and described in a selected time with the help of several independent methods.

Studied materials and samples

Gray gypsum (Gypstrend s.r.o., Czech Republic), hydrated lime labeled as CL-90-S (Carmeuse CR, Czech Republic), and silica fume (Stachesil S produced by Stachema, Czech Republic) as a pozzolan material were used for the

preparation of all studied samples. Lime is necessary for the alkali activation of pozzolan (silica fume) since gypsum does not contain $Ca(OH)_2$. The used silica fume consists of more than 90 mass% of amorphous phases. The reference sample (labeled as R) was prepared from gypsum (90 mass%) and lime (10 mass%). The ternary system gypsum–lime–silica fume (labeled as SF) was designed with the mass content of 81.5, 10, and 8.5 mass%, respectively. Detailed compositions of both mixtures are summarized in Table 1. This unusual proportion was designed according to the previous results described in [12, 21] where the sequential simplex method was used. This method is based on the best-fitting composition of mixtures with the best mechanical properties, for the detailed description (see [12]). The amount of pozzolan depends on the content of amorphous (active) phases in the material. Thus, similarly to the previous research where about 10 mass% of metakaolin was in the ternary gypsum-based system to achieve the best mechanical properties of studied materials after the continuous exposure to water environment, the identical amount of the amorphous phase in the silica fume was used. Therefore, the content of silica fume in the studied samples was chosen as 8.5 mass%.

The chemical composition of the calcined gypsum, lime, and silica fume was verified by the high-resolution X-ray fluorescence method (XRF), namely Thermo ARL 9400 XP (Thermo ARL, Switzerland). The results are summarized in Table 2. It can be seen that lime and silica fume are of very high purity. The calcined gypsum contained mainly SO_3 and CaO. From the X-ray diffraction (XRD) results, it was determined that the gypsum contains bassanite ($CaSO_4 \cdot 1/2H_2O$), anhydrite ($CaSO_4$), kaolinite ($Al_2Si_2O_5(OH)_4$), chamosite, quartz, and traces of muscovite.

The procedure of the samples preparation was as follows: In the case of the reference samples, calcined gypsum and lime hydrate were mixed together. After thorough mixing by hand, the dry mixture was added into the measured amount of water. The mixture was then mixed in a laboratory mixer for 60 s at low speed and another 30 s at higher speed, whipped off, and mixed again for another 60 s at high speed. The mixture was removed from the mixer and put into the molds. After 1 h, the samples were demolded. The samples were prepared with the dimensions of 40 × 40 × 160 mm. In the case of SF samples, silica fume and lime hydrate in dry state were mixed together first. Then, calcined gypsum was added and the composition was mixed again until it was homogenized. The procedure of mixing was the same as in the case of the reference samples. All samples were stored in laboratory conditions for 24 h. After this time, a half of the samples were put in water (labeled as W) and the rest of the samples (labeled as A) were kept in the laboratory conditions (atmospheric air, constant temperature of 25 °C). Before the simultaneous thermal analysis (STA), a small piece was taken from the inner part of the sample. It was dried at the temperature of 50 °C to a constant mass. This temperature was chosen in accordance with the research done by Rovnaníková et al. [23]. It was found that at temperatures higher than 50 °C the chemically bound water could be removed and the material starts to decompose. Then, the part of the sample was ground, and about 50 mg of powder sample was used for STA.

Table 1 Composition of the studied mixtures (in mass%)

Mixture	Gypsum	Lime	Silica fume	Water/mL kg^{-1}
R	90	10	–	700
SF	81.5	10	8.5	730

Experimental

Simultaneous thermal analysis (STA)

Simultaneous thermal analysis consisting of differential scanning calorimetry (DSC) and thermogravimetry (TG) was used to find, analyze, and quantify hydration products, thermal stability, and carbonation levels of all studied samples. The STA was carried out using a Labsys Evo device (Setaram, France). The experiments were done in the temperature range from 25 to 1000 °C in an argon atmosphere with a flow rate of 40 mL min^{-1}. The heating rate was 5 °C min^{-1}. The powder samples with mass about 50 mg were placed in an alumina crucible with a lid.

Evolved gas analysis (EGA)

To support the results obtained from the STA, the EGA was performed by a Simultaneous Setaram Analyser Setsys Evolution 1750 (Setaram, France) coupled with Omnistar Pfeiffer mass spectrometer (Germany). The samples were heated at 10 °C min^{-1} up to 1000 °C in a platinum crucible without a lid under the dynamic argon (99.999% purity) atmosphere with a flow rate of 20 mL min^{-1}.

X-ray diffraction (XRD)

The phase composition of the studied materials was analyzed by XRD method. The X-ray diffraction analysis of the studied mixtures was done after 182 days of hydration using a PANalytical X′PertPRO diffractometer (PANalytical, Spectris plc, Egham, Surrey, England) equipped with

Table 2 Chemical composition of used materials (in mass%)

Component	CaO	SiO_2	MgO	Al_2O_3	SO_3	Fe_2O_3	K_2O	LOI
Gypsum	41.8	6.9	0.7	2.5	45.5	1.0	0.4	1.2
Lime	99.0	0.1	0.7	–	–	–	–	0.2
Silica fume	0.6	94.0	0.3	0.6	0.8	1.9	1.4	0.4

a $Co_K\alpha$ X-ray tube (40 kV, 30 mA). Diffractograms were collected in the range of 2θ 5–41° with a step of 0.017° at 1000 s/step (the scan time 5 h).

Scanning electron microscopy (SEM)

The presence of hydration products, as a result of pozzolanic reaction between silica fume and a system consisting of gypsum and lime, was also proved by scanning electron microscopy. An electron microscope ZEISS Merlin with Gemini II column at acceleration voltage of 7–10 kV, probe current of 46–150 pA, and working distance of 8–15 mm was applied. The InLens detector, which detects the secondary electrons and shows primarily the topography of the surface, was used. The charge compensator was applied due to the low conductivity of the samples. Small pieces were taken from the inner part of dried samples. Before the measurements, they were cleaned by plasma cleaner.

Basic physical properties

The basic physical properties—the bulk density ρ [kg m^{-3}], matrix density ρ_m [kg m^{-3}], and open porosity ψ [%]—of studied samples were measured at the age of 28 days. Before the measurements, the samples stored in both environments were carefully dried to a constant mass. The bulk density was determined by the gravimetric method from the mass and sample dimensions. The open porosity was measured by a mercury intrusion porosimetry using an apparatus Pascal 140 + 440 (Thermo Electron). The matrix density was calculated on the basis of the knowledge of these two parameters [24].

Compressive strength

The development of mechanical properties was studied up to 90 days of hydration. The measurements were realized in order to find whether silica fume is able to compensate the decrease in strength caused by moisture. The compressive strength was measured according to the procedure described in the technical standard ČSN EN 1015 [25]. For the measurement, three prismatic samples for each of the environments and each hydration time were prepared. The measurements of the compressive strength were taken on the halves of broken prisms with a loading area about 1600 mm^2. The uncertainty of the testing method was 1.4% [26].

Results and discussion

Evolution and thermal stability of hydration products

Reference samples

The heat flow and relative mass changes of the reference material R at a given temperature and hydration time are shown in Fig. 1. In Fig. 1, the upper three curves correspond to the samples stored in laboratory conditions (R-A), while the bottom three curves correspond to the samples stored in the water environment (R-W).

There are six more or less significant peaks (see Fig. 1a) referring to the main hydration products. The first and most significant double peak corresponds to the dehydration of gypsum dehydrate to hemihydrate (bassanite) and then to anhydrite. The corresponding chemical reactions may be written as [27]

$$\underset{\text{Gypsum}}{CaSO_4 \cdot 2H_2O} \xrightarrow{\text{1.step(peak)}} \underset{\text{Bassanite}}{CaSO_4 \cdot \frac{1}{2}H_2O} \xrightarrow{\text{2.step(peak)}} \underset{\text{Anhydrite}}{\gamma \cdot CaSO_4}. \quad (3)$$

These reactions take place in the temperature interval from about 60–230 °C. The dehydration of gypsum can be observed also as a one-step process when anhydrite (γ-$CaSO_4$) is directly produced during the gypsum dehydration [28–30] and hemihydrate is formed by rehydration of γ-$CaSO_4$ during cooling in humid air [29, 30]. If the dehydration of gypsum proceeds through one or two steps, it depends on the temperature and partial pressure of water (*P*H2O), differences in crystalline characteristics (size, habit, amounts of defects), impurities and chemical composition of gypsum [31]. For reference sample, the gypsum decomposes in two processes, which can be explained by the use of autogenous *P*H2O atmosphere. The corresponding mass changes at this stage (summarized in Table 3) are consistent with the stoichiometry of the dehydration reactions described in Eq. (3), which confirms the two-step dehydration process.

The peak temperature of the dehydration of gypsum does not change in time, as it was expected. The first step

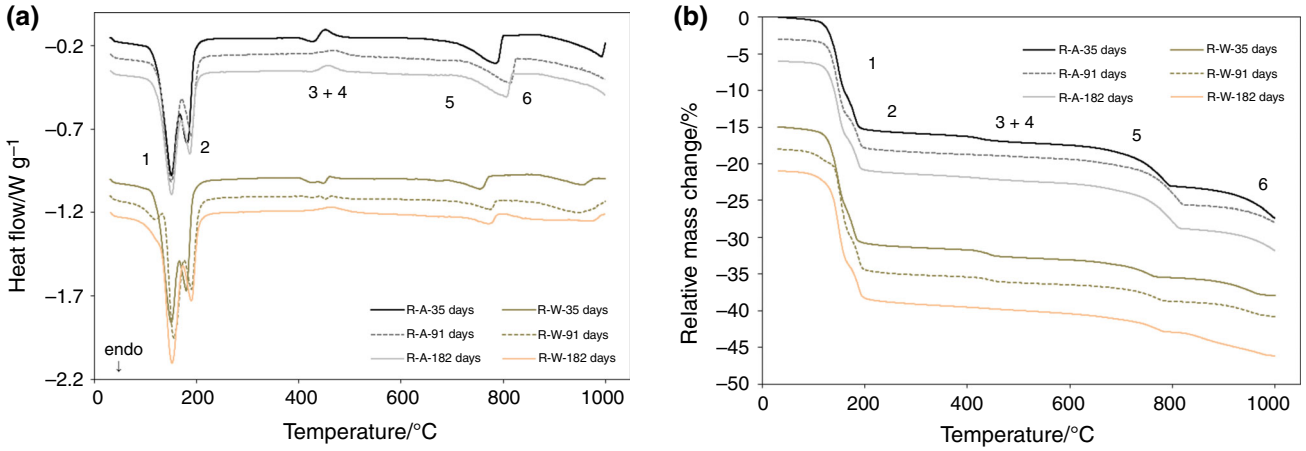

Fig. 1 DSC curves (**a**) and the corresponding mass changes curves (**b**) of the reference materials stored in air in laboratory conditions (R-A) and water environment (R-W) in the age of 35, 91, and 182 days

Table 3 Peak temperatures, mass changes, and enthalpies of the gypsum dehydration for the reference samples

Sample	Time/days	Temperature/°C		Mass change/%	Enthalpy/J g^{-1}
		1	2	1 + 2	1 + 2
R-A	35	149.3	180.1	− 15.4	444.8
	91	149.1	188.3	− 15.0	374.2
	182	150.7	186.5	− 15.0	372.2
R-W	35	150.0	179.5	− 16.0	459.2
	91	154.5	188.6	− 16.7	457.5
	182	151.6	189.6	− 17.4	457.2

of the dehydration (gypsum to bassanite) occurs in the temperature interval from 70 to 166 °C for the samples stored in the laboratory conditions and from 63 to 167 °C for the samples stored in the water environment. The second step of the dehydration of gypsum (bassanite to anhydrite) occurs at temperatures between 166 and 231 °C (laboratory conditions) and 169–231 °C (water environment). The corresponding mass loss of these overlapping reactions was found between 15.0 and 15.4% in the laboratory conditions and between 16.0 and 17.4% in the water environment, respectively (see Fig. 1b, Table 3). The enthalpy was calculated for both steps together, and it is higher for the samples stored in the water environment (R-W), which was also expected (see Table 3). The variety between the results is probably caused by impurities included in the raw materials, mainly in gypsum.

The third peak corresponds to the decomposition of portlandite $Ca(OH)_2$ represented by the endothermal peak, while the fourth peak corresponds to an exothermal reaction that undergoes at the same temperature range and is associated with the transformation of anhydrite. The thermal decomposition of portlandite may be written as

$$Ca(OH)_2 \rightarrow CaO + H_2O. \quad (4)$$

The decomposition of portlandite proceeds at temperatures between 390 and 460 °C, which is in a good agreement with the results in [18] and [32]. The highest temperature of this reaction is observed for the samples stored in the laboratory conditions. The mass change in this temperature interval is small because of the small amount of portlandite in the samples. The mass loss is observed in the R-A samples up to 182 days of hydration (0.7, 0.3, and 0.3% in 35, 91, and 182 days, respectively). In the R-W samples, the changes are visible only for 35 and 91 days of hydration (0.9 and 0.3%, respectively). The exothermal reaction is not accompanied by any mass change, and it is the most significant in the samples stored in the laboratory conditions (see Fig. 1a). In the case of the samples stored in water, the exothermal reaction is not significant, except for the sample with hydration time of 182 days. The amount of portlandite in and after 35 days of hydration is calculated based on its mass loss [33]. For 35 days of hydration, it is higher for the samples stored in the water environment (3.7%) than for the samples stored in the laboratory conditions (2.9%). The portlandite content decreases in time in both reference samples. (It is 1.5% for the R-A sample in 91 and 182 days of hydration and 1.3% for the R-W samples in 91 days of hydration.) After

reaching the age of 182 days, portlandite is not present in the R-W sample anymore. In this temperature interval, another reaction takes place. This reaction corresponds probably to the transformation of anhydrite from a soluble γ-$CaSO_4$ (in the literature it is labeled also as α-$CaSO_4$) into an insoluble ß-$CaSO_4$, and it usually occurs at temperatures about 350–380 °C [27, 34]. In the presented DSC curves, it is observed as an exothermal peak and is shifted to higher temperatures (422–503 °C for the R-A samples and 443–500 °C for the R-W samples, respectively). This shift could be caused by the thermal decomposition of portlandite, which takes place in the same temperature interval. In some papers, it was presented that the anhydride transformation occurs already between 130 and 230 °C, which is probably given by different conditions during experiments (residual vapor pressure of 1 Pa) [35]. The calculation of enthalpy for these reactions is not useful because there are two (exothermal and endothermal) overlapping peaks.

The fifth peak at temperature about 800 °C corresponds to the decomposition of $CaCO_3$, which is a product of lime carbonation [18]. The thermal decomposition of calcite is described as:

$$CaCO_3 \rightarrow CaO + CO_2. \quad (5)$$

The peak temperatures, enthalpies, and mass changes are summarized in Table 4. It is interesting that the temperature of peaks moves to higher values with the age of samples for both environments. The amount of $CaCO_3$ in samples stored in the laboratory conditions is more than two times higher, as it is observed via enthalpies and more significant mass losses, because the carbonation process in water is slower. The enthalpy of the R-A samples is almost the same during the hydration time, and it is between 120.9 and 128.1 J g^{-1}, whereas for the samples stored in water (the R-W samples) it slightly increases from 39.7 to 50.7 J g^{-1}. The content of calcite was calculated from its mass changes [33]. The amount of calcite slightly increases from 12.7 to 14.3% for the R-A samples in time, while for the R-W samples it is almost three times smaller (from 5.2% to 5.9%).

Finally, the last, sixth peak is observed at temperatures above 850 °C. It is caused probably by the decomposition of calcium sulfate ($CaSO_4$) [18, 36],

$$CaSO_4 \rightarrow CaO + SO_3. \quad (6)$$

It is obvious that this reaction is not finished and it continues above the upper temperature limit of 1000 °C.

The results of the STA obtained for the R samples show that the dehydration of the gypsum proceeds in two steps (to bassanite and then to anhydrite). The size of the reaction does not depend on time. A somewhat higher changes of mass are observed for the samples stored in the water environment. The amount of portlandite is higher for the samples stored in water environment, which was expected. The decomposition of portlandite is observed also for the R-W samples in 91 days of hydration. This reaction is not observed after 35 days of hydration for the R-A samples. Nevertheless, the portlandite decomposition peak overlaps with the anhydrite transformation, which takes place almost in the same temperature interval. It seems that the amount of anhydrite is almost constant for the R-A samples during hydration, while for the R-W samples this is not clear because of overlapping portlandite decomposition processes. The calcite content is found to be almost three times higher for the samples stored in the laboratory conditions than for the R-W samples, because carbonation process is faster in air.

Gypsum–lime–silica fume system

The heat flow and relative mass changes obtained from the ternary gypsum-based material labeled as SF at a given temperature and hydration time are shown in Fig. 2. Similarly to the reference samples, in Fig. 2 the upper three curves correspond to the samples stored in air in the laboratory conditions (SF-A). The bottom three curves demonstrate the results of the samples stored in the water environment (SF-W). Also in these results, there are six more or less significant peaks (see Fig. 2a). The differences between reference samples and the gypsum–lime–silica fume system are already obvious from the first peak where the dehydration of gypsum takes place.

Table 4 Peak temperatures, mass changes, and enthalpies of calcite decomposition for reference samples

Sample	Time/days	Temperature/°C	Mass change/%	Enthalpy/J g^{-1}
R-A	35	783.5	− 5.6	128.1
	91	813.0	− 6.2	120.2
	182	806.0	− 6.3	120.9
R-W	35	755.8	− 2.3	39.7
	91	773.5	− 2.3	45.3
	182	772.0	− 2.6	50.7

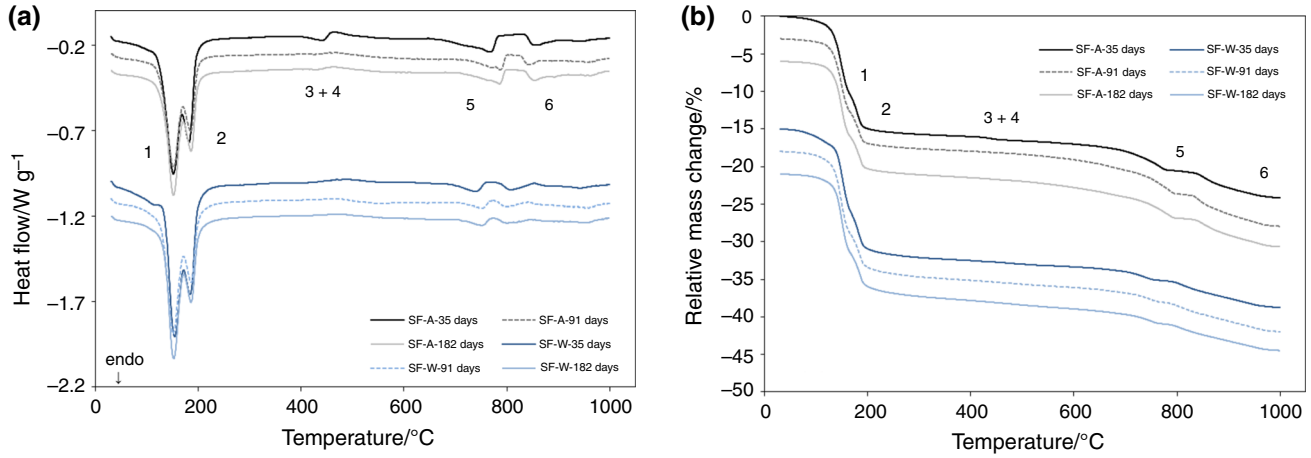

Fig. 2 DSC curves **a** and the corresponding mass changes curves **b** of the ternary gypsum-based materials stored in air in laboratory conditions (SF-A) and water environment (SF-W) in the age of 35, 91, and 182 days

The addition of the pozzolan activates the pozzolanic reaction, and the hydration process is modified. In this case, CSH phases are also produced, which is mostly visible in the enthalpies of the double peaks. The enthalpy of the samples stored in the laboratory conditions decreases in time from 432.5 to 338.8 J g^{-1}, while for the samples stored in the water environment it decreases from 469.6 to 377.0 J g^{-1}. These values are different than those for the reference samples as a consequence of the presence of a material other than gypsum. Since CSH phases are decomposed in the same temperature range, it is difficult to separate them from the dehydration of gypsum. On the other hand, the values of mass changes (see Fig. 2b, Table 5) are almost the same as in the case of the references samples (see Table 4), which also refers to the presence of CSH phases. Therefore, a small amount of gypsum (about 10%) in the SF samples is replaced with something else (CSH phases) to reach the same mass changes as in the R samples. The decreasing trend of the amount of CSH phases is given by the carbonation process, which is slower in the water environment. The presence of CSH phases is challenging to prove by some other techniques. Their structure is amorphous, and therefore, it is not detectible by XRD for example. However, it can be found using a microscopy, which is discussed later.

Similarly to the reference samples, the third and fourth peaks correspond to the decomposition of portlandite $Ca(OH)_2$ and the anhydrite transformation from soluble γ-$CaSO_4$ to insoluble ß-$CaSO_4$ (see above). The portlandite decomposition is observed only for the samples stored in the laboratory conditions. The amount of $Ca(OH)_2$ was determined for 35 and 91 days of hydration (1.9 and 0.8%, respectively). It is not observed for the S-A sample at 182 days of hydration. For the S-W samples, the portlandite content is negligible, and thus, $Ca(OH)_2$ has been consumed by the pozzolanic reaction. The peak temperatures of the anhydrite transformation for the SF-A samples are similar to the reference samples (from 463 to 466 °C), while they are shifted to higher values for the samples stored in water (from 474 to 485 °C). The enthalpy of the SF-A samples during aging is lower than that of the reference samples (from 11.7 to 9.5 J g^{-1}). Nevertheless, it is slightly higher for the SF-W samples (from 5.9 J g^{-1} to 8.9 J g^{-1}), which can be due to the absence of portlandite in the structure of the samples. Therefore, this reaction is better visible, because it is not overlapping with the portlandite decomposition.

Table 5 Peak temperatures, mass changes, and enthalpies of gypsum dehydration and CSH phases decomposition for the SF samples

Sample	Time/days	Temperature/°C		Mass change/%	Enthalpy/J g^{-1}
		1	2	1 + 2	1 + 2
SF-A	35	151.5	182.4	− 15.3	432.5
	91	150.6	184.3	− 14.2	338.8
	182	151.6	186.0	− 14.4	341.4
SF-W	35	152.0	182.7	− 16.6	469.6
	91	151.1	186.1	− 16.3	381.6
	182	152.1	186.0	− 15.6	377.0

Finally, there are interesting peaks at temperatures above 700 °C which are overlapping. The peak, labeled as 5 in Fig. 2a, corresponds to the decomposition of $CaCO_3$, which is a product of the carbonation of lime and hydration products. Since portlandite was consumed during the hydration process, these peaks are smaller than in the case of the reference samples. The peak temperature shifts to lower values for both samples in comparison with the reference sample, as it is shown in Table 6. The enthalpy decreases in time for both samples: from 64.2 to 38.0 J g^{-1} for the SF-A samples, and from 17.1 to 12.7 J g^{-1} for the SF-W samples. As it was already mentioned, the differences are also given by the fact that the carbonation process is slower in water. Therefore, the mass loss is in good agreement with these results. From the calculated calcite content based on its mass losses [33], it is clear that the addition of silica fume slows down the carbonation process even in the laboratory conditions. (It decreases from 7.3% to 6.4% with time.) It is the same for the SF-W samples during aging (2.9%).

It is challenging to identify the peaks which occur at temperatures above 800 °C without any further analysis. As it was already discussed in the case of the reference samples, the last endothermic peak is probably caused by the decomposition of calcium sulfate ($CaSO_4$). However, it seems that also an exothermal reaction occurs in this temperature interval. It can be associated with the products formed in the presence of silica fume [37]. A calcium inosilicate mineral called wollastonite ($CaSiO_3$) may be formed when $CaCO_3$ and SiO_2 are exposed to higher temperatures [38],

$$CaCO_3 + SiO_2 \rightarrow CaSiO_3 + CO_2. \quad (7)$$

This component was observed also in the case of blended concretes containing silica fume [39–43] when similar conditions of thermal analysis were applied. This particular reaction was specified by the EGA.

The STA results of the SF samples indicate that the pozzolanic reaction was activated. Similarly to the results of the R samples, the dehydration of the gypsum proceeded via two steps, but also the decomposition of CSH phases took place in the same temperature interval. It is proven by almost the same mass changes of all studied samples stored in both environments. (The amount of gypsum in the SF samples is lower by 10%, so the expected mass loss would be also lower without CSH phases present in the structure.) Similarly to the R samples, the size of the reaction is not dependent on time, while more significant mass changes are observed for the samples stored in the water environment. However, the presence of CSH phases needs to be proved by some other techniques, such as SEM, which will be discussed. Next, portlandite is found in the SF-A samples up to 182 days of hydration, as for the R-A samples. On the other hand, it is not observed in the SF-W samples (in the R-W samples it was visible up to 91 days of hydration), which means that $Ca(OH)_2$ was probably consumed by the pozzolanic reaction. The enthalpies of the anhydrite transformation of the SF-A samples are by about 4% lower than in the case of the R-A samples, while the values for the SF-W are slightly higher than for the R-W samples on an average. The calcite content is slightly lower in the SF samples stored in both environments than in the reference samples. The content is constant in the SF-W samples during aging, which indicates a positive effect of silica fume (and water) on the durability of the samples. It is also given by the fact that portlandite is consumed during the hydration process, and it could not participate in the carbonation processes anymore. Note that the results on the calcite decomposition are also influenced by the exothermic reaction of the wollastonite crystallization, which occur in the same temperature interval.

EGA results

For a better understanding of the processes occurring in the studied materials especially at higher temperatures, the EGA of the ternary gypsum-based samples was also performed (see Fig. 3). It shows that molecules of H_2O liberate from the sample in the temperature interval from 50 to 250 °C and from 390 to 430 °C, which corresponds to the dehydration processes and the decomposition of portlandite. CO_2 releases from the sample in the temperature range from 500 to 800 °C where the calcite decomposition is presented, which is in good agreement with the DSC and TG results. Above 800 °C, the liberation of CO_2, SO_2, and SO takes place. Therefore, it can be concluded that the

Table 6 Peak temperatures, mass changes, and enthalpies of calcite decomposition for the SF samples

Sample	Time/days	Temperature/°C	Mass change/%	Enthalpy/J g^{-1}
SF-A	35	768.3	− 3.2	64.2
	91	787.0	− 3.0	38.2
	182	786.0	− 2.8	38.0
SF-W	35	739.5	− 1.3	17.1
	91	752.0	− 1.3	14.2
	182	752.5	− 1.3	12.7

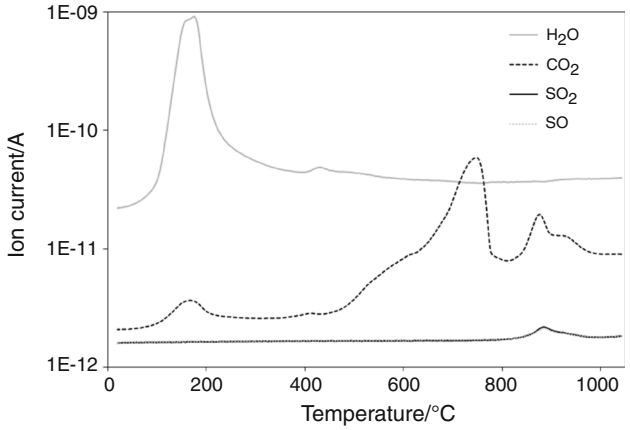

Fig. 3 EGA curves of the ternary gypsum-based material stored in air in laboratory conditions (SF-A)

wollastonite crystallization and $CaSO_4$ decomposition occur in this temperature interval as it was supposed and described above.

Portlandite content and carbonation process

The mineralogical phases of the studied samples after 182 days of hydration were determined by the X-ray diffraction method to find and quantify the hydration products. These results are summarized in Table 7. (The amount of amorphous phase was not calculated.) The amounts of gypsum, basanite, and anhydrite correspond to their typical behavior if they are placed in water. The portlandite content is found to be 1.7% in the R-A samples and 0.3% for the SF-A samples, which is in good agreement with the measurements taken by the STA (1.5 and 0%, respectively). On the other hand, small differences are probably caused by the overlapping thermal decomposition of the portlandite and anhydrite transformation, which occur in the same temperature interval. The portlandite was not observed at samples stored in water. These results are in accordance with the STA and show that the addition of silica fume supports the pozzolanic reaction.

Table 7 Phase composition of studied materials after 182 days of hydration (in mass%)

Component	Chemical formula	R-A	R-W	SF-A	SF-W
Gypsum	$CaSO_4{\cdot}2H_2O$	42.1	74.2	43.1	77.2
Bassanite	$CaSO_4{\cdot}0.5H_2O$	27.0	11.1	24.5	6.2
Anhydrite	$\gamma{\cdot}CaSO_4$	8.1	1.4	10.6	1.7
Portlandite	$Ca(OH)_2$	1.7	–	0.3	–
Calcite	$CaCO_3$	11.2	5.5	12.7	7.5
Quartz	SiO_2	3.9	3.4	4.1	3.2
Muscovite	$KAl_2(AlSi_3O_{10})(OH)_2$	6.0	4.4	4.7	4.2

The amount of calcite which refers to the carbonation level in the studied materials was verified. The results of both methods are relatively similar. The XRD method detected 11.2 and 5.5 mass% of calcite in the structure of R-A and R-W samples, respectively, while in the case of the STA it was 14.3 and 5.9 mass%, respectively. These results demonstrate that materials stored in water are protected against carbonation. The same trend was observed in the case of the ternary gypsum-based materials where it was observed that the addition of silica fume slows down the carbonation process even when stored in the laboratory conditions (see Fig. 4). The calcite content in the SF-A was more than a half lower than in the R-A samples after 182 days.

Besides the main hydration products, also some minor phases were found by the XRD method. All the studied samples contained quartz and muscovite, which came mainly from the used gypsum. It should be noted that the CSH phases are not detected by XRD although their presence as a product of pozzolanic reaction was expected. It is caused by the fact that CSH phases have mainly amorphous structure, which is not detectable by XRD. The amount of the amorphous phase was not evaluated so these numbers represent only the total amount of all mineralogical phases present in the structure.

CSH phases observed by SEM method

The presence of CSH phases was confirmed by SEM observations (see Fig. 5). While in the case of the reference samples stored in water, mainly crystals of gypsum and calcite can be observed, in the case of samples with silica fume, also CSH phases are visible in picture.

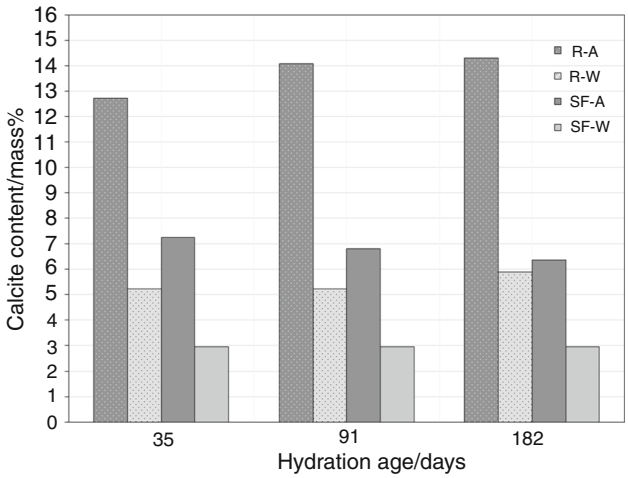

Fig. 4 Level of carbonation determined from the STA results in a time horizon up to 182 days of hydration

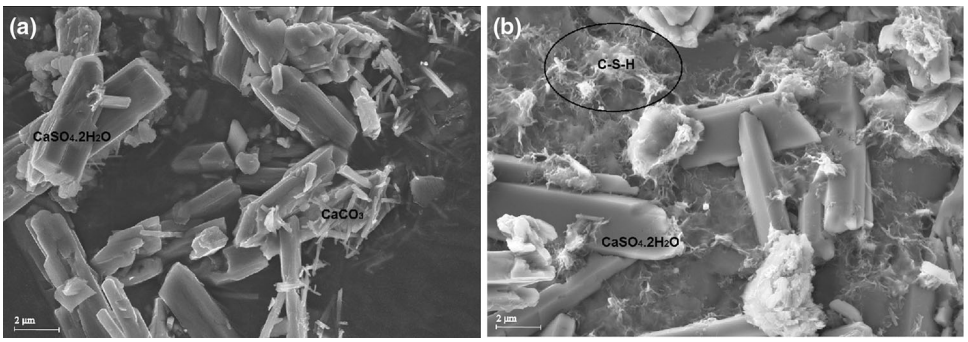

Fig. 5 SEM photographs of the reference sample samples **a** and the ternary gypsum-based materials **b** stored in water environments and measured in the age of 182 days

Basic physical properties

To provide the complex information about the studied materials, also the basic physical properties were determined. The summary of these results measured at the age of 28 days of hydration is given in Table 8. The bulk density of the reference samples stored in the laboratory condition (R-A) is 1062 kg m^{-3}, which is higher by about 2.5% than the bulk density for the sample stored in the water environment (R-W). The bulk density of the SF samples is almost the same for both environments (996 kg m^{-3} and 995 kg m^{-3}, respectively), which is lower by about 6.2% than the value for the R-A sample. The matrix density for the reference samples in the water environment is smaller (by about 20.9%) than for the R-A sample, whereby no products of pozzolanic reactions are expected. In the case of the SF samples, the matrix density increased in the water environment in comparison with the laboratory conditions (by about 11.6%). A denser microstructure refers to the pozzolanic reactions occurring in the structure of the SF samples. This is also supported by the results of the pore distribution curves already deeply discussed in [11, 22]. The samples stored in the water environment had smaller pores than the samples stored in the laboratory conditions. The results of the open porosity show that the R-W sample has its lowest value. The structure of the sample without pozzolan is coarser, because no pozzolanic products were formed. The moisture properties (such as water transport) at the age of 28 days were also determined and are discussed in [22]. It was found out that the samples with pozzolan stored in the water environment (SF-W) have a finer pore structure, which has a positive effect on water transport properties.

Compressive strength

The results on the compressive strength up to 90 days of hydration are summarized in Fig. 6. The performance of all studied materials was found to be very similar after 7 days of curing regardless of the environment where the samples were stored. After 28 days of hydration, the reference samples stored in water have lower values of the compressive strength in comparison with the samples with the silica fume. A similar trend was observed after 90 days of hydration. The results for the reference samples confirmed the typical behavior of gypsum, since the compressive strength decreases with moisture of the samples. The compressive strength of the SF-W samples after 90 days increases approximately twice, which shows a positive effect of the water environment on the pozzolanic reactions and stability of the hydration products of studied samples. In the previous research [44], the influence of moisture on the compressive strength of various ternary gypsum-based binders was discussed also in relation to different pretreatments before testing (drying × not drying samples before procedures). It was found out that the SF samples have a lower compressive strength in the dry state in comparison with the reference samples, but their strength is higher if they are suited in wet environments.

Table 8 Basic physical properties of studied samples (after 28 days of hydration) stored in laboratory conditions (A) and in the water environment (W)

Mixture	Storage	Bulk density/kg m^{-3}	Matrix density/kg m^{-3}	Open porosity/%
R	A	1062	2578	59.2
	W	1036	2039	49.2
SF	A	996	2218	55.1
	W	995	2475	59.8

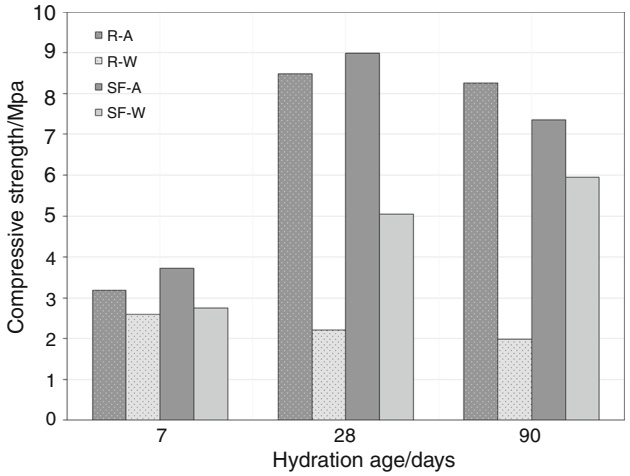

Fig. 6 Mechanical properties of studied materials stored in laboratory conditions (**A**) and in the water environment (W) within a time horizon of 90 days

Conclusions

In this paper, a possible utilization of gypsum-based materials in wet environment was studied. A system containing of gypsum, lime, and silica fume was stored under laboratory conditions in air and water. The influence of silica fume on the performance of the newly designed system was studied and compared with a reference material consisting only of gypsum and lime. Some selected properties were measured in a time up to 182 days of hydration. The results obtained in this study can be summarized as follows:

- The pozzolanic reaction was activated by the addition of silica fume. It can be documented with the presence of CSH phases which were successfully detected via SEM photographs. These phases were indirectly seen also on the thermogravimetry results.
- The portlandite was consumed at samples with silica fume by the pozzolanic reaction already after 35 days of hydration, and it was not observed in the samples with the age of 91 days which also refers to the positive influence of the silica fume addition on this reaction.
- The carbonation level was lower for samples stored in the water environment, as it was expected. However, in the case of samples with silica fume, the samples were preserved even in laboratory conditions. It implies that silica fume can even protect the samples against carbonation (up to 182 days).
- From the results of the compressive strength measurements, it can be concluded that the reference samples has the lowest performance in the water environment, while the samples enriched with silica fume show even an increase in strength in time.

The results also show that in contrary to gypsum itself, newly designed gypsum-based ternary binders with silica fume exhibit a good performance in the wet environment. Therefore, their properties should be studied more extensively because these materials have a potential to be used for the production for lightweight materials for thermal insulation boards, renovation and fireproof mortars or it can be prepared in the form of light-weighted blocks for load-bearing walls with thermal insulation properties.

Acknowledgements This research was supported by the Czech Science Foundation, Project No. GA16-01438S and by Project No. SGS16/199/OHK1/3T/11.

References

1. Garg M, Jain N, Singh M. Development of alpha plaster from phosphogypsum for cementitious binders. Constr Build Mater. 2009;23(10):3138–43.
2. Just A, Schmid J, König J. Gypsum plasterboards used as fire protection-Analysis of a database. Stockholm: SP Technical Research Institute of Sweden; 2010.
3. Değirmenci N. Utilization of phosphogypsum as raw and calcined material in manufacturing of building products. Constr Build Mater. 2008;22(8):1857–62.
4. Fauziah I, Zauyah S, Jamal T. Characterization and land application of red gypsum: a waste product from the titanium dioxide industry. Sci Total Environ. 1996;188(2–3):243–51.
5. Gazquez MJ, Bolivar JP, Vaca F, García-Tenorio R, Caparros A. Evaluation of the use of TiO_2 industry red gypsum waste in cement production. Cem Concr Compos. 2013;37:76–81.
6. Bhanumathidas N, Kalidas N. Dual role of gypsum: set retarder and strength accelerator. Indian Concr J. 2004;78(3):1–4.
7. Kumar S. Fly ash-lime-phosphogypsum cementitious binder: a new trend in bricks. Mater Struct. 2000;33(1):59–64.
8. Marinkovic S, Kostic-Pulek A. Examination of the system fly ash–lime–calcined gypsum–water. J Phys Chem Solids. 2007;68(5–6):1121–5.
9. Shen W, Zhou M, Zhao Q. Study on lime–fly ash–phosphogypsum binder. Constr Build Mater. 2007;21(7):1480–5.
10. Demir I, Serhat Baspinar M. Effect of silica fume and expanded perlite addition on the technical properties of the fly ash–lime–gypsum mixture. Constr Build Mater. 2008;22(6):1299–304.
11. Doleželová M, Vimmrová A. Porosity of the ternary gypsum-based binders with different types of Pozzolan. Key Eng Mater. 2016;677:122–7.
12. Vimmrová A, Keppert M, Michalko O, Černý R. Calcined gypsum–lime–metakaolin binders: design of optimal composition. Cem Concr Compos. 2014;52:91–6.
13. Tsantaridis LD, Östman BAL, König J. Fire protection of wood by different gypsum plasterboards. Fire Mater. 1999;23(1):45–8.
14. Leiva C, García Arenas C, Vilches LF, Vale J, Gimenez A, Ballesteros JC, Fernández-Pereira C. Use of FGD gypsum in fire resistant panels. Waste Manage. 2010;30(6):1123–9.
15. Li J, Zhuang X, Leiva C, Cornejo A, Font O, Querol X, Moeno N, Arenas C, Fernández-Pereira C. Potential utilization of FGD gypsum and fly ash from a Chinese power plant for manufacturing fire-resistant panels. Constr Build Mater. 2015;95:910–21.
16. Saulnier V, Durif S, Bouchaïr A, Audebert P, Lahmar M. Experimental studies of unprotected and protected steel structures under fire. In: Applications of structural fire engineering

(proceedings of the international conference in Dubrovnik). Prague:CTU; 2017.
17. Doleželová M, Scheinherrová L, Krejsová J, Vimmrová A. Effect of high temperatures on gypsum-based composites. Constr Build Mater. 2018;168:82–90.
18. Tydlitát V, Trník A, Scheinherrová L, Podoba R, Černý R. Application of isothermal calorimetry and thermal analysis for the investigation of calcined gypsum–lime–metakaolin–water system. J Therm Anal Calorim. 2015;122(1):115–22.
19. Doleželová M, Krejsová J, Vimmrová A. Temperature resistance of the ternary gypsum-based binder with microsilica. AIP Conf Proc. 2016;1752:040003.
20. Doleželová M, Scheinherrová L, Vimmrová A. Moisture resistance and durability of the ternary gypsum-based binders. Mater Sci Forum. 2015;824:81–7.
21. Vimmrová A, Doleželová M, Černý R. Ternary gypsum based materials with improved mechanical properties. Stavební Obzor. 2014;7–8:126–31 **[in Czech]**.
22. Doleželová M, Čáchová M, Scheinherrová L, Vimmrová A. Effect of pozzolan on the physical properties and the moisture properties of the gypsum-based binders. Central Europe towards Sustainable Building 2016; Prague: Grada Publishing; 2016. pp. 1049–54.
23. Rovnaníková P, Bayer P, Krmíčková N. Effect of higher temperature on properties of gypsum. In: Sádra 2005. Brno:VUT Brno; 2005. pp. 39–43 [in Czech].
24. Antepara I, Pavlík Z, Žumár J, Pavlíková M, Černý R. Properties of hydrophilic mineral wool for desalination of historical masonry. Mater Sci-Medzg. 2016;22(1):88–93.
25. No EN. 1015, Methods of test for mortar for masonry—Part 11: Determination of flexural and compressive strength of hardened mortar. Prague: Czech Standardization Institute; 2000.
26. Pavlík Z, Keppert M, Pavlíková M, Žumár J, Fořt J, Černý R. Mechanical, hygric, and durability properties of cement mortar with MSWI bottom ash as partial silica sand replacement. Cem Wapno Beton. 2014;19(2):67–80.
27. Couturier J. Method for producing an anhydrite III or α based hydraulic bonding agent. Google Patents US6706113 B1; 2004.
28. Carbone M, Ballirano P, Caminiti R. Kinetics of gypsum dehydration at reduced pressure: an energy dispersive X-ray diffraction study. Eur J Mineral. 2008;20(4):621–7.
29. Prasad P, Krishna Chaitanya V, Shiva Prasad K, Narayana Rao D. Direct formation of the γ-CaSO4 phase in dehydration process of gypsum: in situ FTIR study. Am Miner. 2005;90(4):672–8.
30. Chio CH, Sharma SK, Muenow DW. Micro-Raman studies of gypsum in the temperature range between 9 and 373 K. Am Miner. 2004;89(2–3):390–5.
31. Lou W, Guan B, Wu Z. Dehydration behavior of FGD gypsum by simultaneous TG and DSC analysis. J Therm Anal Calorim. 2011;104(2):661–9.
32. Zelić J, Rušić D, Krstulović R. Kinetic analysis of thermal decomposition of $Ca(OH)_2$ formed during hydration of commercial Portland cement by DSC. J Therm Anal Calorim. 2002;67(3):613–22.
33. Dweck J, Buchler PM, Coelho ACV, Cartledge FK. Hydration of a Portland cement blended with calcium carbonate. Thermochim Acta. 2000;346(1–2):105–13.
34. Clifton JR. Thermal analysis of calcium sulfate dihydrate and supposed a and b forms of calcium sulfate from 25 to 500 C. J Res Natl Bur Stand A: Phys Chem. 1972;76A(1):41–9.
35. Badens E, Llewellyn P, Fulconis J, Jourdan C, Veesler S, Boistelle R, et al. Study of gypsum dehydration by controlled transformation rate thermal analysis (CRTA). J Solid State Chem. 1998;139(1):37–44.
36. Kuusik R, Salkkonen P, Niinistö L. Thermal decomposition of calcium sulphate in carbon monoxide. J Therm Anal. 1985;30(1):187–93.
37. Esteves LP. On the hydration of water-entrained cement–silica systems: combined SEM, XRD and thermal analysis in cement pastes. Thermochim Acta. 2011;518(1–2):27–35.
38. Zhu H, Newton R, Kleppa O. Enthalpy of formation of wollastonite ($CaSiO_3$) and anorthite ($CaAl_2Si_2O_8$) by experimental phase equilibrium measurements and high-temperature solution colorimetry. Am Miner. 1994;79(1–2):134–44.
39. Trník A, Scheinherrová L, Kulovaná T, Reiterman P, Vejmelková E, Černý R. Thermal analysis of high-performance mortar containing burnt clay shale as a partial portland cement replacement in the temperature range up to 1000°C. Fire Mater. 2017;41(1):54–64.
40. Palou MT, Kuzielová E, Novotný R, Šoukal F, Žemlička M. Blended cements consisting of Portland cement–slag–silica fume–metakaolin system. J Therm Anal Calorim. 2016;125(3):1025–34.
41. Palou MT, Šoukal F, Boháč M, Šiler P, Ifka T, Živica V. Performance of G-Oil Well cement exposed to elevated hydrothermal curing conditions. J Therm Anal Calorim. 2014;118(2):865–74.
42. Trník A, Scheinherrová L, Medved' I, Černý R. Simultaneous DSC and TG analysis of high-performance concrete containing natural zeolite as a supplementary cementitious material. J Therm Anal Calorim. 2015;121(1):67–73.
43. Trník A, Fořt J, Pavlíková M, Čáchová M, Čítek D, Kolísko, Černý R, Pavlík Z. UHPFRC at high temperatures–Simultaneous thermal analysis and thermodilatometry. AIP Conference proceedings. 2016;1752:040028.
44. Doleželová M, Vimmrová A. Moisture influence on compressive strength of ternary gypsum-based binders. AIP Conference proceedings; 2017: AIP Publishing.